Noname manuscript No.
(will be inserted by the editor)

A tale of two cities

A comparative study of London and Paris public transit fragility

Christian von Ferber · Bertrand Berche · Taras Holovatch · Yurij Holovatch

Received: date / Accepted: date

Abstract We present a comparative analysis of changes that occur in the city public transit networks due to random failures or targeted attacks of different nature that cause malfunctioning of its constituents – stations or links (rails, roads, etc.) that connect them. We show how does accumulation of such changes lead to the emergent phenomena that cause break of the transportation system as a whole. Simulating different directed attack strategies, we derive vulnerability criteria that result in minimal strategies with high impact. As a case study, we choose London and Paris public transit networks. Our quan-

Christian von Ferber
Applied Math. Research Centre Dep. of Mathematics, Coventry University, Coventry, CV1 5FB, UK & Theoretische Physik II, Heinrich-Heine-University Düsseldorf, D-40225 Germany
Tel.: +44-24-7688-8560
Fax: +44-24-7688-8585
E-mail: aa2374@coventry.ac.uk

Bertrand Berche
Statistical Physics Group, Institut Jean Lamour, Université de Lorraine, BP 70239, F-54506 Vandœuvre les Nancy, France
Tel.: +33 383 68 48 15
Fax: +33 383 68 48 01
E-mail: Bertrand.Berche@ijl.nancy-universite.fr

Taras Holovatch
Applied Math. Research Centre Dep. of Mathematics, Coventry University, Coventry, CV1 5FB, UK & Statistical Physics Group, Institut Jean Lamour, Université de Lorraine, BP 70239, F-54506 Vandœuvre les Nancy, France
Tel.: +44-24-7688-8560
Fax: +44-24-7688-8585
E-mail: holovatch@gmail.com

Yurij Holovatch
Institute for Condensed Matter Physics, National Academy of Sciences of Ukraine, Lviv, UA-79011 Ukraine
Tel.: +38 032 2760908
Fax: +38 032 2761158
E-mail: hol@icmp.lviv.ua

titative analysis is performed in the frames of the complex network theory – a methodological tool that has emerged recently as an interdisciplinary approach that joins methods and concepts of random graph theory and statistical physics.

Keywords public transit · attack vulnerability · complex networks · percolation

PACS 02.50.-r · 07.05.Rm · 89.75.Hc

Mathematics Subject Classification (2000) MSC code1 · MSC code2 · more

1 Introduction

Charles Dickens famous novel who's title is used to name this article starts one of its chapters with the words "The traveller fared slowly on his way, who fared towards Paris from England in the autumn of the year one thousand seven hundred and ninety-two. More than enough of bad roads, bad equipages, and bad horses, he would have encountered to delay him" [1]. In those times, there was perhaps not too much difference neither between the quality of transportation systems in the two countries, nor between typical reasons that cause its malfunctioning. Although, different historical circumstances caused additional impact on traveling security. In our days, general believe is that again on average not too much difference is observed between facilities offered by transportation networks of developed countries. However, available digital databases together with computer-based technologies and analytical approaches allow to quantify the difference and to make a comparative case study.

The goal of this paper is to compare certain features of the contemporary public transit - public transportation networks (PTN) - of two European capitals, London and Paris. These cities were chosen both because of a lot of similarities in their structure and functioning caused by geographical and social reasons as well as because of a special attraction payed nowadays to public facilities of London as a capital of the Olympic games 2012. In particular we will be interested in the reaction of PTN on random failures or targeted attacks of different nature that cause malfunctioning of is constituents – stations or links (rails, roads, etc.) that connect them. A comprehensive analysis of such problem needs simultaneous consideration of both the PTN load (i.e. traffic and passenger flows) and the PTN structure (i.e. topological properties of a network). Although being feasible in principle, such a task needs an essential numerical effort and an access to numerous databases of different origin. Here, we will make only a first but essential step to reach this goal. Namely, we will consider only the PTN structure and analyze how fragile are the structures of London and Paris PTN to failure of their constituents. As we will see below, already such comparison allows to make certain conclusions and predictions about robustness of PTN and their behaviour under attacks of different nature.

The setup of this paper is as follows. In the next section we will briefly describe the method of our analysis – complex network theory [2,3] – and overview some relevant studies where this method has already been applied to analyze transportation networks of different types. We will start discussing problem of PTN fragility in section 3, there we will show how such problem is related to the percolation theory [4] and introduce observables that allow to give a quantitative measure of PTN change under attack. This problem we be further analyzed in section 4. There, we will make comparative analysis of London and Paris PTN and of their changes under attacks of different types. We will conclude by section 5, where we will discuss possible reasons for differences in PTN robustness and offer criteria that allow to judge about PTN robustness prior to attack.

2 PTN seen as a complex network

An observation that lines of a public transit routes of a city form a network and that this network is a complex enough one is a part of our everyday experience. However, a new sense has been given to a notion of *complex network* recently: complex network theory is a new and rapidly developing field of knowledge that has its routes in random graph theory and statistical physics (see e.g. recent reviews [2] and monographs [3]). From mathematical point of view, a network is nothing else but a graph with a set of edges and a set of vertices as its constituents. Graph theory is well-settled branch of discrete mathematics that originates from the classical XVIII century works of L. Euler [5]. An essential breakthrough and a paradigm shift in graph (and in particular in random graph) theory occurred in 90-ies of last century, when from an analysis of single small graphs and properties of individual vertices or edges (or as we will name them below of nodes and links) the task of the research shifted to consideration of statistical properties of graphs (or networks). It was realized, that numerous natural and man-made structures have a form of a network and that these networks posses amazing properties, strikingly different from those of the so-called classical random graph. Such networks are currently known as complex networks. To name a few, to them belong metabolic, ecological, social, internet, www, transportation and many networks more. Complex networks were found to be compact structures (sometimes called *small worlds*) with short distance between nodes, high level of correlations and self-organization. They demonstrate extremely high robustness if their constituents are removed at random, however they are vulnerable to targeted attacks. Certain their properties are governed by power laws, which would signal about non-trivial correlations present in their structure. We set out to show that similar properties are inherent to the PTN of London and Paris we are interested in our study.

Table 1 Some characteristics of the PTNs analyzed in this study. N: number of stations; R: number of routes. The following characteristics are given: $\langle k \rangle$ (mean node degree); $\ell^{\max}$, $\langle \ell \rangle$ (maximal and mean shortest path length); $\mathcal{C}$ (relation of the mean clustering coefficient to that of the classical random graph of equal size, (3)); $\mathcal{C}^b$: betweenness centrality (5); $\kappa^{(z)}$, $\kappa^{(k)}$ (c.f. Eqs. (15), (14)); γ (an exponent in the power law (4) fit. More data is given in [11].

City	N	R	$\langle k \rangle$	$\ell^{\max}$	$\langle \ell \rangle$	$\mathcal{C}$	$\mathcal{C}_B$	$\kappa^{(z)}$	$\kappa^{(k)}$	γ
London	10937	922	2.60	107	26.5	320.6	$1.4 \cdot 10^5$	1.87	3.22	4.48
Paris	3728	251	3.73	28	6.4	78.5	$1.0 \cdot 10^4$	5.32	6.93	2.62

In general, there exists already a bulk of research [6–12] that gives quantitative evidences of the fact that the PTNs share general features of other transportation networks like the airport, railway, or power grid networks [2]. These features include evolutionary growth, optimization, and usually an embedding in two dimensional (2D) space. First numerical studies of PTNs in frames of the complex network theory often were devoted to analysis of certain sub-networks of city transit. Examples are given by the subways of Boston [6, 7], Vienna [7] and some other cities [8], city buses in Poland [9] and China [10]. However, as far as the bus-, subway- or tram-subnetworks are no closed systems the inclusion of additional subnetworks has significant impact on the overall network properties as has been shown for the subway and bus networks of Boston [6]. Therefore, in further analysis of PTN all such subnetworks were taken into account [11].

Two PTN analyzed within our study are either operated by a single operator (Traffic for London, TFL) or by small number of operators with a coordinated schedule (three operators for Paris), as expressed by a central web site from which our data was obtained.[1] The analyzed PTN of London covers metropolitan area of 'Greater London' and includes buses, subway, and tram. Correspondingly, the PTN of Paris which was the subject of our analysis covers the metropolitan area 'aire urbaine' and comprises buses, RER and subway. Some characteristics of these networks are given in Table 1. Currently, different ways to represent a PTN in a form of a graph are exploited [6–13]. In what follows below, we will use the so-called **L**-space representation [6, 9, 11], when a public transport station is represented by a vertex (node) of a graph and two stations are connected by an edge (link) when there is at least one PTN rout that successively goes through them. In such representation the obtained graph – complex network – is most similar to the PTN map.[2] Typical size of the network is usually evaluated on the base on $\ell^{\max}$ and $\langle \ell \rangle$, the maximal and mean *shortest path length*. The latter is defined by:

$$\langle \ell \rangle = \frac{2}{N(N-1)} \sum_{i>j} \ell(i,j), \qquad (1)$$

[1] See [11] for a more detailed description of the database.
[2] Note, however that multiple links are absent in this graph.

where N is the number of network nodes, $\ell(i,j)$ is the length of a shortest path from node i to j and the sum spans all pairs i,j of sites of the network. Comparatively low values of $\langle \ell \rangle$ for the PTN under consideration (see Table 1) bring about their small world structure [11]. Larger value of $\ell^{\max}$ for the PTN of London corresponds to the larger area covered by the network (as seen, e.g. from larger number of routes and stations).

The mean and maximal shortest path lengths characterize the network as a whole and sometimes are referred to as the global properties of a network. An example of a local property is given by a node degree k_i, a number of links that are connected to the node i. By definition, it is equal to the number of nodes adjacent to the given one and defines the neighbourhood size of a node i. Apparently, not all nearest neighbours of the node i are the nearest neighbours of each other. Their relative number is given by a *clustering coefficient*:

$$C_i = \frac{2y_i}{k_i(k_i-1)}, \quad k_i \geq 2, \tag{2}$$

where y_i is the number of links between node i neighbors and $C_i = 0$ for $k_i = 0, 1$. In general, clustering reflects specific form of correlation present in a network: the clustering coefficient of a node also gives the probability of any two of its randomly chosen neighbors to be connected. A useful numerical indicator is given by a relation of the mean clustering coefficient of a network to that of the classical Erdös-Rényi random graph of equal size:

$$\mathcal{C} = \langle C_i \rangle / C_{ER}, \tag{3}$$

with $C_{ER} = 2M/N^2$. The classical Erdös-Rényi random graph is constructed by completely random linking of N nodes by M links [2,3]. Therefore, the high values of $\mathcal{C}$ given in Table 1 bring about presence of strong correlations in the networks under consideration. Moreover, London PTN appears to possess stronger correlation properties than that of Paris.

Another striking difference between the properties of the random graph and of the PTN under consideration is given by behaviour of the node-degree distribution $P(k)$, probability that arbitrary chosen node is of degree k. Whereas the random graph is characterized by Poissonian distribution, and therefore, by an exponential decay at large k [2,3], it was empirically observed in [11] that for PTN of London and Paris corresponding distribution function decays due to the power law:

$$P(k) \sim k^{-\gamma}, \quad k \gg 1. \tag{4}$$

The power law decay (4) bring about the *scale-free* properties of London and Paris PTN. It is instructive to note already here, that the exponent γ governing this decay is much smaller for the PTN of Paris, see Table 1. As will become evident later, this fact has certain consequences for the network fragility.

To some extent, the node degree may be considered as a local measure of the node importance: intuitively it is clear that hubs play essential role in a complex network. The importance of a node with respect to the connectivity between other nodes of the network is measured by the *betweenness centrality*.

For a node i, the latter measures the share of the shortest paths between nodes that this node mediates and is defined as:

$$\mathcal{C}_B(i) = \sum_{j \neq i \neq k} \frac{\sigma_{jk}(i)}{\sigma_{jk}} \tag{5}$$

where σ_{jk} is the number of shortest paths between nodes j and k and $\sigma_{jk}(i)$ is the number of these paths that go via node i. Numerical values of the mean betweenness centrality are given in Table 1 for the PTN under consideration. In what follows below we will be interested also in the other centrality measures, these will be explained in section 3.

3 PTN fragility: observables and attack scenarios

Studies of complex network behaviour at removal of their constituents (nodes or links) have much in common with studies of lattice percolation phenomenon [4]. However, the latter occurs on homogeneous structures (lattices) whereas the non-homogeneity of complex networks gives rise to a variety of phenomena which are particular for these structures. Empirical analysis of numerous scale-free real-world networks gave numerous evidences that these networks display an unexpectedly high degree of robustness under random failure [2,3]. However they are especially vulnerable to the attacks, that target certain important network constituents. As we have seen in the previous section, the PTN under consideration share many common features of complex networks, therefore it is natural to expect similarities in their behaviour during attack of different scenarios.

On a lattice, it is the appearance of the spanning cluster that signals an onset of percolation at given concentration $c_{\rm perc}$ of the lattice constituents (nodes or links). In turn, the probability that an arbitrary chosen lattice site belongs to the spanning cluster is naturally used as an order parameter: it is equal one at $c = 1$, zero at $c = c_{\rm perc}$ and varies between these two values for $c_{\rm perc} \leq c \leq 1$. Similar to percolation phenomenon occurs when the giant connected component (GCC) emerges on an idealized complex network. The GCC is defined as a connected subnetwork which in the limit of an infinite network contains a finite fraction of the network. Strictly speaking, the GCC is absent for any real-world complex network because of its finite size. Therefore, to monitor changes in the network structure when certain concentration of its nodes (links) c is removed one often uses the normalized largest components size, defined as:

$$S(c) = N_1(c)/N, \tag{6}$$

where N and N_1 are the numbers of nodes in the initial network and in its largest component, correspondingly. Another 'order-parameter-like' variable used to judge about the changes in network structure is the mean inverse shortest path length [14]:

$$\langle \ell^{-1} \rangle = \frac{2}{N(N-1)} \sum_{i>j} \ell^{-1}(i,j). \tag{7}$$

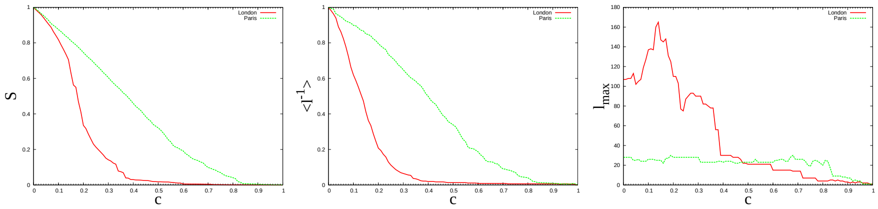

a. **b.** **c.**

Fig. 1 Size of the largest component S (**a**), mean inverse $\langle \ell^{-1} \rangle$ (**b**) and maximal $\ell^{\max}$ (**c**) shortest path length as function of the removed nodes concentration c for PTN of London (red curve) and Paris (green curve). Random removal of PTN nodes/stations.

Here, as in (1), $\ell(i,j)$ is the shortest path between nodes i and j. Note however, that opposite to (1) which is ill-defined for the disconnected network, quantity (7) is well-defined as far as $\ell^{-1}(i,j) = 0$ if nodes i, j are disconnected. Therefore it can be used to trace changes of network behavior under attack.

In Figs. 1 **a**, **b** we show the behaviour of S and $\langle \ell^{-1} \rangle$ for the PTN of London (red curve) and Paris (green curve) as function of the concentration of removed nodes c, when these nodes were removed at random. Already this first attempt to model PTN behavior under attack brings about higher fragility of London PTN to random removal of its nodes/stations: indeed both the S- and $\langle \ell^{-1} \rangle$-curves manifest faster decay in the case of London PTN. Moreover, the S-curve for the Paris PTN decays almost linearly, that signals that network clusterization is almost absent and the largest component decreases only due to the nodes removal. This observation will be further quantified in the next section. Here, we want to support it by displaying the maximal shortest path length behaviour, Fig. 1 **c**. As a matter of fact, $\ell^{\max}$ manifests very different behaviour for these two PTN. For London PTN, $\ell^{\max}$ grows initially and then, when a certain threshold is reached ($c \sim 0.14$) it abruptly decreases. Obviously, removing the nodes initially increases the path lengths as deviations from the original shortest paths need to be taken into account. Further removing nodes then at some point leads to the breakup of the network into smaller components on which the paths are naturally limited by the boundaries which explains the sudden decrease of their lengths. Such peculiarities in $\ell^{\max}$ behaviour are almost not observed for Paris PTN, at least for small and medium values of c.

Note, that plots of Fig. 1 display results of a single sequence of nodes random removing. As we have checked by repeating the random attack sequence [13,15], due to the large PTN size a 'self-averaging' effect takes place: averaging over many random attack sequences instances do not significantly modify the plots presented in Fig. 1. To further analyze the PTN attack vulnerability, we have made a series of computer simulations removing the PTN constituents not only at random, but also according to certain prescriptions aimed to single out the most (or the less-) important nodes. Several more indicators were used besides the node degree, betweenness centrality (5), and clustering coefficient (2). Beneath them, we used the number of the next nearest neighbours adjacent to the node, z_2, as well as the closeness $C_C(j)$, graph $C_G(j)$, and stress centralities, defined as follows [16]:

$$C_C(j) = \frac{1}{\sum_{t \in \mathcal{N}} \ell(j,t)}, \tag{8}$$

$$C_G(j) = \frac{1}{\max_{t \in \mathcal{N}} \ell(j,t)}, \tag{9}$$

$$C_S(j) = \sum_{s \neq j \neq t \in \mathcal{N}} \sigma_{st}(j). \tag{10}$$

Here, again $\ell(j,t)$ is the length of a shortest path between the nodes j, t that belong to the network $\mathcal{N}$, σ_{st} is the number of shortest paths between the two nodes $s, t \in \mathcal{N}$, and $\sigma_{st}(j)$ is the number of shortest paths between nodes s and t that go through the node j. One more attack scenario was prompted to us by studies of immunization problems on complex networks [17]. It consists in removing of a randomly chosen neighbor of a randomly chosen node and is based on the fact, that in this way nodes with a high number of neighbors will be selected with higher probability. Each of the above described scenarios (except of the random ones) was realized for the lists prepared for the initial network or rebuilt by recalculating the order of the remaining nodes after each step. The last way is known to be usually more effective and leads to slightly different results suggesting that the network structure changes in the course of the attack [14, 18].

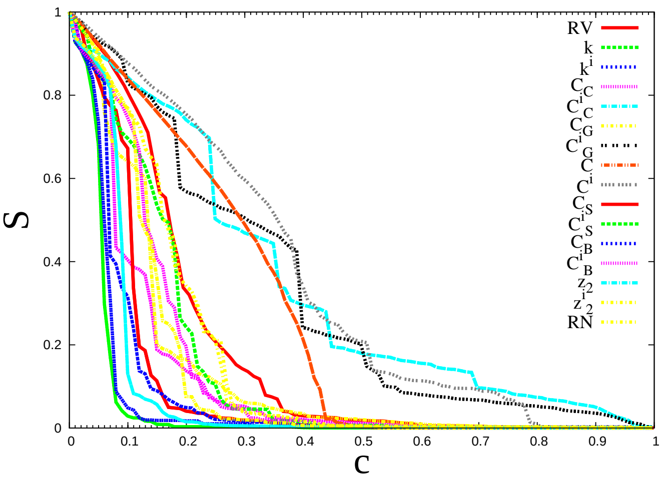

Fig. 2 Size of the largest component of London PTN at removal of nodes according to the lists ordered by the decreasing node degree k, closeness $\mathcal{C}_C$, graph $\mathcal{C}_G$, stress $\mathcal{C}_S$, betweenness $\mathcal{C}_B$ centralities, number of second nearest neighbors z_2, increasing clustering coefficient $\mathcal{C}$. The lists were prepared for the initial PTN before the attacks (denoted by a superscript i) or rebuilt by recalculating the order of the remaining nodes after each step (without superscript). RV, RN: random removal of a node or of its randomly chosen neighbour.

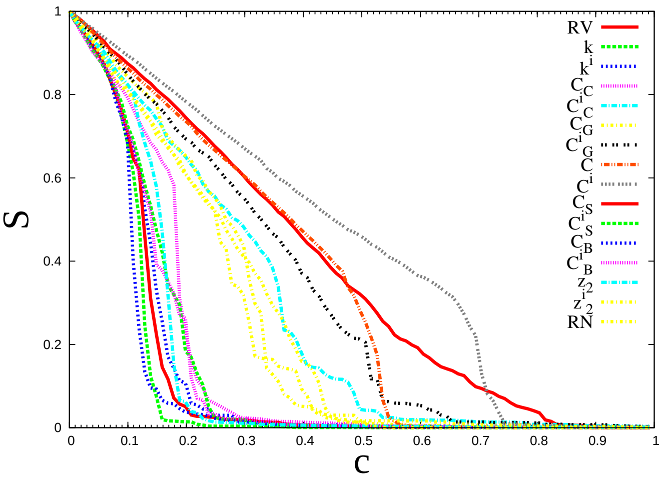

Fig. 3 Size of the largest component of Paris PTN for different attack scenarios. Notations the same as in Fig. 3

In Figs. 2, 3 we show the changes in the size of the largest component of London and Paris PTN at removal of nodes according to all sixteen attack scenarios described above. More specifically, for the scenarios based on the recalculated node lists, instead of recalculating the PTN characteristics after the removal of each individual node, the nodes were removed in groups of 1 % of the initial nodes and the PTN characteristics were recalculated after the removal of each such group. As it follows from the first glance on the plots, the most harmful are attacks targeted on the nodes of highest node degree, highest betweenness and closeness centralities, highest second nearest neighbours number. We will discuss them in more details in the next section, completing the picture of node-targeted attacks by that of attacks that target PTN links.

4 PTN fragility: quantitative analysis

In this section, we are going to discuss in more details reaction of PTN on most harmful attacks and to compare them with the random attack scenario. To this end, we will introduce the variable that allows to quantify PTN robustness [19, 20]. Furthermore, we will seek for correlations between the PTN characteristics prior to the attack and its robustness during attacks of different type. This agenda will be followed first for the node-targeted attacks (section 4.1) and then for the link-targeted ones (section 4.2).

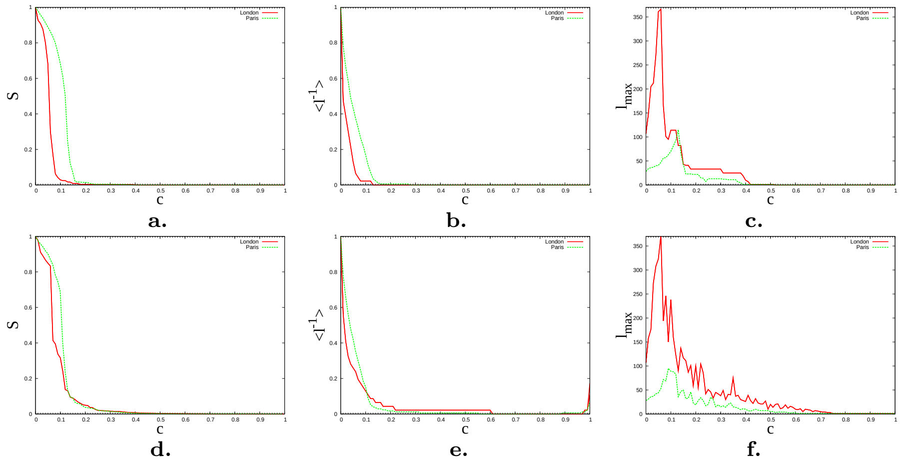

Fig. 4 Size of the largest component S, mean inverse $\langle \ell^{-1} \rangle$ and maximal $\ell^{\max}$ shortest path length as function of the removed nodes concentration c for PTN of London (red curve) and Paris (green curve). **a**, **b**, **c**: recalculated highest node degree scenario. **d**, **e**, **f**: recalculated highest betweenness centrality scenario.

4.1 Node-targeted attacks

As it is clearly seen from Figs. 2, 3, scenarios when the nodes are removed in the order of their decreasing degree or decreasing betweenness centrality belong to those that cause most harm to the PTN: decrease of S is fast and it becomes almost zero at the concentration of removed nodes $c \sim 0.2 \div 0.3$. In Fig. 4 we further detail this picture giving plots for the size of the largest component S, mean inverse $\langle \ell^{-1} \rangle$ and maximal $\ell^{\max}$ shortest path length as function of the removed nodes concentration c for recalculated highest node degree (figures **a** – **c**) and recalculated highest betweenness centrality (figures **d** – **f**) scenarios. Comparing them with the corresponding plots of Fig. 1, where an impact of the random nodes removing is shown, one concludes that the behaviour of both PTN is not as different as it was observed for the random scenario. Although at the recalculated highest node degree scenario both $S(c)$ and $\langle \ell^{-1}(c) \rangle$ curves manifest faster decay for London PTN (see Figs. 4 **a**, **b**), the difference is less pronounced in the case of the recalculated highest betweenness centrality scenario (Figs. 4 **d**, **e**). Similarity in both PTN performance at such attacks follows also from the observation of the maximal shortest path length $\ell^{\max}$ behaviour. Pronounced peaks in $\ell^{\max}(c)$ first occur at $c \sim 0.06$ and $c \sim 0.1$ for London and Paris PTN correspondingly and then are repeated with certain periodicity giving an ample evidence of clusterization phenomena in both networks.

The above comparison of PTN attack fragility was to a large extent a qualitative one. To proceed further with quantitative analysis, one has to introduce a numerical measure of such fragility. In the percolation theory, when a spanning cluster occurs abruptly at the percolation concentration c_{perc}, the latter gives and example of such measure. In the case of real-world networks of finite size one has rather to speak about the region of concentrations where an emergent behaviour of fast performance decay occurs. Sometimes the characteristic concentration value based on peculiarity in S, $\langle \ell \rangle$, $\langle \ell^{-1} \rangle$ or $\ell^{\max}$ is used [14,15]. From now on let us focus on the behaviour of the PTN largest component. Below, we will use the measure that allows to capture the network reaction over the whole attack sequence [19]. For the normalized size $S(c)$ of the largest component as function of concentration c let us define the area A below the $S(c)$ curve by:

$$A = 100 \int_0^1 S(c)\mathrm{d}c, \tag{11}$$

and use this as a measure of the PTN robustness. As follows from the definition (11), the measure captures the effects on the network over the complete attack sequence, it is an integral characteristics and is well-defined for a finite-size network.

Table 2 Fragility measure A, (11), for the PTNs of London and Paris. Columns 2-6 give the value of A for node-targeted attacks, columns 7-11 give A for link-targeted attacks. See the text for attack scenario description.

City	Node-targeted attacks					Link-targeted attacks				
	RV	k	k^i	$\mathcal{C}_B$	$\mathcal{C}_B^i$	RL	$k^{(l)}$	$k^{i,(l)}$	$\mathcal{C}_B^{(l)}$	$\mathcal{C}_B^{i,(l)}$
London	29.31	5.45	6.28	8.71	14.17	27.45	20.95	22.85	27.2	27.33
Paris	37.93	10.77	13.12	10.67	14.07	56.04	47.12	51.83	55.93	48.03

In the left part of table 2 we give the value of of A for the highest node degree and highest betweenness scenarios (performed according to the initial and to the recalculated node lists, correspondingly) and compare them with the random scenario. As it follows from the table, almost in all instances Paris PTN shows better performance (higher value of A) as that of London. Another conclusion concerns the difference between value of A for the random attack (RV) and for the attacks that target influential nodes (with high degree k or high betweenness centrality $\mathcal{C}_B$): as it is usual for the complex networks, they are robust during random removal of their constituents and especially vulnerable to targeted attacks. A natural question arises whether such result can be anticipated: can one make some conclusions about PTN fragility prior to the attack? Indeed, the data of table 1 where information about initial PTN characteristics is summarized allow at least qualitatively to predict an outcome of attacks summarized in table 2. To show this, below we shortly recall several facts known from the complex network theory.

In has been shown [21,22], that a GCC on an uncorrelated infinite network is present if:

$$\langle k(k-2) \rangle \geq 0. \tag{12}$$

Relation (12) often is referred as the Molloy-Reed criterion. Defining the Molloy-Reed parameter as the ratio

$$\kappa^{(k)} = \langle k^2 \rangle / \langle k \rangle, \tag{13}$$

one may rewrite (12) as:

$$\kappa^{(k)} \geq 2. \tag{14}$$

As it was illustrated for many real-world PTN [13,15,20], the value of Molloy-Reed parameter for the unperturbed network may be used also to judge about network fragility during attack. Typically, the networks with lower $\kappa^{(k)}$ appear to be more vulnerable to random and node degree-targeted attacks. This observation was further supported by monitoring another parameter, defined by the relation of the mean second neighbours number z_2 to the mean neighbours number z_1:[3]

$$\kappa^{(z)} = z_2 / z_1. \tag{15}$$

It is easy show that $\kappa^{(k)} = \kappa^{(z)} + 1$ for uncorrelated networks. However, as we have seen from the analysis of section 2, strong correlations are present in the PTN, therefore one can not expect a simple relation between parameters (14), (15). Rather, comparison of $\kappa^{(z)}$ for two given networks will provide additional information about their relative robustness.

We have calculated values of $\kappa^{(k)}$ and $\kappa^{(z)}$ for London and Paris PTN and give them in the ninth and tenth columns of table 1. Corresponding values for Paris PTN exceed more than twice those for London bringing a clear signal about higher vulnerability of London PTN to random failures. This conclusion has been empirically demonstrated in simulations reported above.

Another evidence about possible higher robustness of Paris PTN with respect to that of London is obtained from comparison of the node-degree distribution exponents γ for both networks (the last column of table 1). The smaller value of γ for Paris PTN corresponds to the fat-tailed node-degree distribution $P(k)$. For an infinite network, the GCC is always present if $\gamma < 3$ [22] and small value of γ for a finite-size network signals about its high robustness as well.

An analysis performed so far concerned attacks, which were targeted on the network nodes. Before passing to general conclusions, let us analyze reaction of the PTN under consideration on the link-targeted attacks.

4.2 Link-targeted attacks

Out of different possible scenarios described in section 3, we will concentrate here on those, which were the most harmful at the node-targeted attacks removing the highest degree and highest betweenness centrality nodes. Our goal will be to check how fragile are the PTN to attacks of similar scenarios with only one but essential modification: what happens when PTN links are

[3] Which is by definition equal to the mean node degree $\langle k \rangle$.

removed instead of PTN nodes? However, to proceed we need to generalize both notions for the case of links. Let us define the degree $k^{(l)}$ of the link between nodes i and j with degrees k_i and k_j as [13,20]:

$$k_{ij}^{(l)} = k_i + k_j - 2. \tag{16}$$

With such definition, the link degree $k^{(l)} = 0$ for the graph with two vertices and a single link, whereas for any link in a connected graph with more than two vertices the link degree will be at least one, $k^{(l)} \geq 1$. The generalization of betweenness centrality is straightforward:

$$\mathcal{C}_B^{(l)}(i) = \sum_{s \neq t \in \mathcal{N}} \frac{\sigma_{st}(i)}{\sigma_{st}}, \tag{17}$$

where σ_{st} is the number of shortest paths between the two nodes $s, t \in \mathcal{N}$, that belong to the network $\mathcal{N}$, and $\sigma_{st}(i)$ is the number of shortest paths between nodes s and t that go through the link i (c.f. formula (5) for the node betweenness centrality). By definition, $\mathcal{C}_B^{(l)}(i)$ measures the importance of a link i with respect to the connectivity between the nodes of the network.

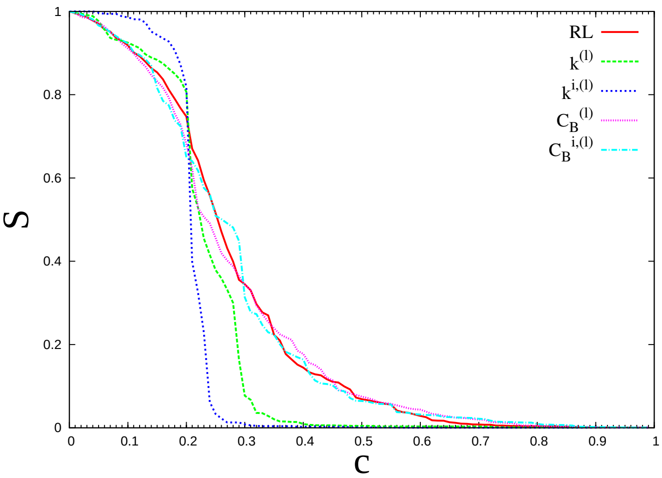

Fig. 5 Size of the largest component of the London PTN for different attack scenarios. Opposite to the Figs. 1 – 4, in this figure and in Fig. 6 the links (not the nodes!) were removed. Therefore, here c means share of removed links.

In Figs. 5, 6 we show results of our simulations of five different attack scenarios, when the PTN links were removed at random (RL) or according to the lists ordered by decreasing link node degrees and link betweenness centrality. As in the case of node-targeted attacks these lists were prepared either prior to the attack (corresponding legends in the figures hold the superscript i: $k^{i,(l)}$, $\mathcal{C}_B^{i,(l)}$) or were recalculated each time when 1% of nodes was removed ($k^{(l)}$,

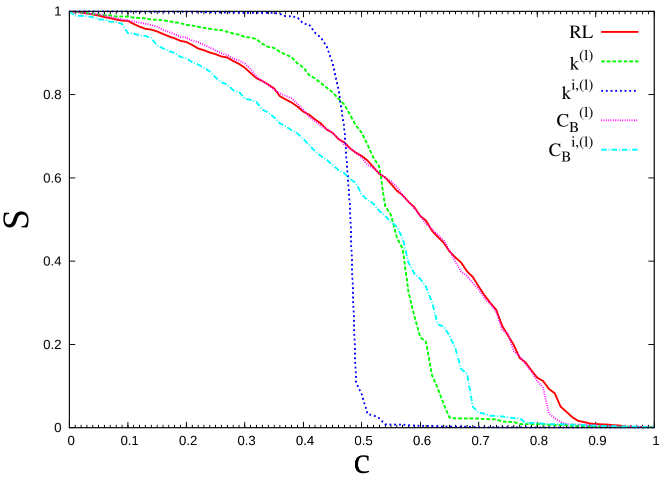

Fig. 6 Size of the largest component of the Paris PTN for different link-targeted attack scenarios as function of concentration of removed links.

$\mathcal{C}_B^{(l)}$). The figures show dependence of the PTN largest component on the concentration of removed links. Let us first note that removal of a link does not necessarily lead to decrease of S, indeed as we see from the figures S remains unchanged for small enough value of c, depending on the attack scenario. This is opposite to the node-targeted attacks, when removal of a node decreased the size of S at least by relative share of this node. In this respect, the most particular behaviour is observed for the highest link degree scenario (blue and green curves in Figs. 5, 6). The value of S first remains practically unchanged (up to the concentration of removed links $c \sim 0.08$ for London PTN and even $c \sim 0.36$ for Paris PTN) and then abruptly decreases almost to zero: behaviour very similar to that observed at lattice percolation [4]! To further detail an impact of different scenarios we have calculated the value of the measure A, introduced in the previous section, see Eq. (11). It is quoted for all five scenarios in the right hand side part of the table 2. As one can see from the table, almost for all link-targeted scenarios the value of A is almost twice larger for Paris PTN in comparison with the London one. Another obvious observation is that different scenarios applied to the same PTN lead to the close values of A. Returning back to Figs. 5, 6 one can further assure that not only the impact but also the $S(c)$ curves demonstrate very similar behaviour at random, and highest link betweenness targeted scenarios.

The above observation that also for the link-targeted attacks London PTN seems to be more vulnerable as Paris one is based on the numerical simulations of certain attack scenarios. Again, as in the former subsection one may be interested if such prediction may be done prior to the attack, on the base of the information about unperturbed network? In our former analysis [13, 20] we have suggested, that a useful criterion to compare fragilities of PTN at link-targeted attacks is to compare the mean node degrees $\langle k \rangle$ of unperturbed networks. Typically, the network with a higher mean node degree is more robust. Moreover, as we have observed for an instance of fourteen different PTN of the major cities of the world [13,20], the measure A calculated for each single network linearly increases with $\langle k \rangle$. This demonstrates correlation of the network stability with the initial 'density' of network links, without relation to the correlations in the PTN structure. To some extent this is different to the criteria discussed in the former subsection for the node-targeted attacks, where the correlations where considered by analyzing the second moment of the node degree distribution $\langle k^2 \rangle$ or its z_2 neighbourhood, that enter the Molloy-Reed parameters (13), (15). Comparing $\langle k \rangle$ for two unperturbed PTN (table 1) one can see that its value for Paris PTN exceeds that for London PTN almost in 1.4 times (2.60 for London and 3.73 for Paris, see the table). This observation may be used as a possible prediction for different attack fragility of these two PTN.

5 Ideas for conclusions and outlook

– if indeed we have not taken some stations for the Paris network into account and if we will take them into account in future, we do not expect this to decrease the PTN stability. Rather we expect that the stability will increase. These additional nodes will rather correspond to local buses in the suburb area. On the one hand, such bus lines either give rise to additional 'unimportant' nodes, that will help to hide hubs at the random scenario. On the other hand, if such lines will connect also the hubs, this will again only improve overall robustness.

Acknowledgements We thank Ralph Kenna for numerous encouraging discussions and for suggesting the title for this paper. This work was supported in part by the 7th FP: IRSES projects 269139 "Dynamics and cooperative phenomena in complex physical and biological environments" and 295302 "Statistical physics in diverse realizations".

References

1. Charles Dickens. A Tale of Two Cities. Chapter 31.
2. R. Albert, A.-L. Barabási, Rev. Mod. Phys. **74**, 47 (2002); S. N. Dorogovtsev, J. F. F. Mendes, Adv. Phys. **51**, 1079 (2002); M. E. J. Newman, SIAM Review **45**, 167 (2003).
3. D. J. Watts, *Small Worlds.* Princeton University Press, Princeton, NJ (1999); S. N. Dorogovtsev, S. N. Mendes, *Evolution of Networks.* Oxford University Press, Oxford (2003); M. E. J. Newman, A.-L. Barabási, D. J. Watts, *The Structure and Dynamics of Networks.* Princeton University Press, Princeton (2006).
4. D. Stauffer, A. Aharony, *Introduction to Percolation Theory.* Taylor & Francis, London (1991).
5. S. Bornholdt, H. Schuster (Eds.), *Handbook of Graphs and Networks.* (Wiley-VCH, Weinheim (2003).
6. M. Marchiori, V. Latora, Physica A **285**, 539 (2000); V. Latora, M. Marchiori, Phys. Rev. Lett. **87**, 198701 (2001); V. Latora, M. Marchiori, Physica A **314**, 109 (2002).
7. K. A. Seaton, L. M. Hackett, Physica A **339**, 635 (2004).

8. P. Angeloudis, D. Fisk, Physica A **367**, 553 (2006); S. Derrible, C. Kennedy, Transportation **37**, 275 (2010); S. Derrible, C. Kennedy, Physica A **389**, 3678 (2010).
9. J. Sienkiewicz, J. A. Holyst, Phys. Rev. E **72**, 046127 (2005); J. Sienkiewicz, J. A. Holyst, Acta Phys. Polonica B **36**, 1771 (2005).
10. P.-P. Zhang, K. Chen, Y. He, T. Zhou, B.-B. Su, Y. Jin, H. Chang, Y.-P. Zhou, L.-C. Sun, B.-H. Wang, D.-R. He, Physica A **360**, 599 (2006); X. Xu, J. Hu, F. Liu, L. Liu, Physica A **374**, 441 (2007); H. Chang, B.-B. Su, Y.-P. Zhou, D.-R. He, Physica A **383**, 687 (2007); Z.-T. Zhu, J. Zhou, P. Li, X.-G. Chen, Chinese Physics B **17**, 2874 (2008).
11. C. von Ferber, Yu. Holovatch, V. Palchykov, Condens. Matter Phys. **8**, 225 (2005); C. von Ferber, T. Holovatch, Yu. Holovatch, V. Palchykov, Physica A **380**, 585 (2007); C. von Ferber, T. Holovatch, Yu. Holovatch, V. Palchykov, Eur. Phys. J. B **68**, 261 (2009).
12. S. Derrible, C. Kennedy, Transport Reviews 1-25 (2011).
13. T. Holovatch, Complex Transportation Networks: Resilience, Modelling and Optimisation, Ph.D. thesis, Nancy University, France & University of Coventry, GB (2011). http://tel.archives-ouvertes.fr/tel-00652784/fr/
14. P. Holme, B. J. Kim, C. N. Yoon, S. K. Han, Phys. Rev. E **65**, 056109 (2002).
15. B. Berche, C. von Ferber, T. Holovatch, Yu. Holovatch, Eur. Phys. J. B **71**, 125 (2009); B. Berche, C. von Ferber, T. Holovatch, Yu. Holovatch, Dynamics of Socio-Economic Systems **2**, 42 (2010).
16. U. Brandes, J. Math. Sociology, **25**, 163 (2001).
17. R. Cohen, S. Havlin, D. ben-Avraham, Phys. Rev. Lett. **91**, 247901 (2003).
18. M. Girvan, M. E. J. Newman, Proc. Natl. Acad. Sci. USA **99**, 7821 (2002).
19. C. M. Schneider, T. Mihaljev, S. Havlin, H. J. Herrmann, preprint arXiv:1102.1929v1 (2011); C. M. Schneider, A. A. Moreira, J. S. Andrade, Jr., S. Havlin, H. J. Herrmann, Proc. Natl. Acad. Sci. USA **108**, 3838 (2011).
20. B. Berche, C. von Ferber, T. Holovatch, Yu. Holovatch. Advances in Complex Systems (to appear), preprint arXiv:1201.5532v1 (2012).
21. M. Molloy, B. A. Reed, Random Struct. Algorithms **6(2/3)**, 161 (1995); M. Molloy, B. Reed, Combinatorics, Probability and Computing **7**, 295 (1998)
22. R. Cohen, K. Erez, D. ben-Avraham, S. Havlin, Phys. Rev. Lett. **85**, 4626 (2000) D. S. Callaway, M. E. J. Newman, S. H. Strogatz, D. J. Watts, Phys. Rev. Lett. **85**, 5468 (2000).